# Supporting Information

## Baker et al. 10.1073/pnas.1114214109

### SI Materials and Methods

**Reagents and Constructs.** Antibodies to CXCR4-PE (2B11), CD3 (OKT3), CCL-19Fc, CD44-APC (IM7), CD4-FITC (RM4-4), and IgG (Fcg specific)-PE from eBioscience; CD11a-FITC (I21/7) and C3G (C-19) from Santa Cruz; IgG-Alexa 488 and anti-mouse IgG-HRP from Invitrogen; CD16/32, CD18-PE (M18/2), CD29-PE (HMb1-1), and CXCR4 (12G5) from Biolegend; and CD4-APC (RM4-5), CD3 (2C11), CD28 (37.51), CD45-PE (RA3/6B2), CD62L-peCy7 (Mel-14), and CD69-peCy7 (H1.2F3) from BD Biosciences. mAb AL57 was provided by M. Shimaoka (Harvard University, Cambridge, MA) and CalDAG–GEFI was provided by A. Graybiel (Massachusetts Institute of Technology, Cambridge, MA). FTY720 (Cayman Chemicals) was injected i.p., 1 mg/kg, and anti-CD62L (Mel-14) antibody was prepared from hybridoma (ATCC). RT-PCR probes for GAPDH, CD3d, RhoH, and IL-2 along with cDNA synthesis kit were from Applied Biosystems. The pRaichu–Rap1 FRET construct was provided by H. Matsuda (Osaka University, Osaka, Japan), and RhoH, from the cDNA resource center at the University of Missouri, was attached to the C terminus of mRFP from pmRFP plasmid courtesy of Roger Tsien (University of California, San Diego, CA).

**Preparation of Cells and Transfection Conditions.** Primary T cells were isolated from whole blood by the polymorph layering technique. The lymphocyte layer was cultured for 3 d in RPMI 1640 containing 10% (vol/vol) FBS and 1 mg/mL PHA (Remel) and then cultured in the presence of 10 ng/mL IL-15 (R&D Systems) for 4–7 d. Mouse CD4 T cells were isolated from spleen and lymph node suspensions by negative selection using the complement method to greater than 90% $CD4^+$. Cell sorting was done for $CD4^+$ $CD44^{low}$ cells to enrich for naïve CD4 cells. Cell sorting was done using a FACSVantage cell sorter (BD Biosciences). Flow cytometry staining was performed at 4 °C for 30 min in PBS with 2.5% FBS, secondary antibody was incubated at 4 °C for 10 min, and fluorescent signal assessed on a FACSCalibur or LSRII (BD Biosciences). Data analysis was done using FlowJo (Tree Star). T-cell blasts from DO11.10 or OT-II were generated by mixing T cells with irradiated BALB/c splenocytes, 1:10 ratio, and 2 mg/mL $OVA_{323–339}$. Retrovirus was generated using the Ecotropic Phoenix cell line (G. Nolan, Stanford University, Stanford, CA) and murine T cells were transduced 1 d after activation.

Amaxa transfection of pcDNA, RhoH–mRFP, mRFP only, or pRaichu Rap1 was done using the Human and Mouse T-cell kits (Lonza) per manufacturer's protocol, with $5 \times 10^6$ cells and 5 mg of DNA. Transfected human cells were supplemented with IL-15 after 3 h and incubated overnight, whereas mouse cells were incubated 8–12 h. RhoH–mRFP and mRFP expressing stable cell lines and transient transfections into Jurkat cells were generated by electroporation at 250 mV and 960 mFD with 75 mg of cDNA.

**Immunoprecipitation and Western Blotting.** Transiently transfected Jurkat cells expressing mRFP or RhoH–mRFP were stimulated for indicated times with CXCL12 (100 nM) or CD3 (3 mg/mL) in L15 + glucose and subsequently lysed as previously described (1) using MLB buffer. Murine T cells were rested in IMDM 1% FBS for 1 h then stimulated with 100 nM CCL21 or CD3 (2 mg/mL) and SA (2.5 mg/mL). Active Rap1A and -B were immunoprecipitated using the Rap1 assay reagent (Ral GDS–RBD) per manufacturer protocol (Millipore). Another fraction of the sample was also assayed by Western for total Rap1 and b-actin to confirm equivalent loading.

**T-cell Adhesion, Migration, and Imaging.** ICAM-1 adhesion was performed as described in ref. 1. Cells were stimulated at 37 °C with CXCL12 or with OKT3 and secondary antibody to induce T-cell receptor (TCR) cross-linking similar to Rap1 assay. Cells were allowed to adhere to an ICAM-1–coated plate at 37 °C, washed, fixed, and then numbers of adhered cells were counted. Rap1 FRET sensor transfected T cells were added to delta T dishes (Fisher Scientific) previously coated with human tonsil CXCL-12 (2 μg/mL) and/or ICAM-1 (6 μg/mL) for 12 h at 4 °C and for 4 h at RT. Approximately $5 \times 10^4$ T lymphocytes were washed and added to a delta T dish containing 1 mL of L-15 medium with 2 mg/mL glucose. Dynamic FRET efficiency was calculated as described previously from Rap1 FRET sensor transfected cells on ICAM-$1^{-/+}$ CXCL12 (2). Image acquisition was conducted on an epifluorescence microscope (TE2000-U microscope; Nikon) using 10–20× objectives coupled to a CoolSNAP HQ CCD (Roper Scientific). Analysis of active LFA-1 was done on fixed cells that had migrated 20 min on CXCL12 and ICAM-1–coated coverslips at 37 °C by staining with AL57. For migration of naïve mouse T cells, dishes were coated overnight at 4 °C with 20 mg/mL protein A and either CXCL12 (2 mg/mL) or CCL21 (4 mg/mL) (R&D), and then incubated with 10 mg/mL ICAM-1Fc for 2 h at RT. Differential interference contrast (DIC) images were acquired every 5 s for 30 min under 10–20× objective lens and 37 °C was maintained throughout the experiment. Meandering index is the displacement/path length and the closer to 1 the number is, the more directional the cell migrates. Migration analysis was performed using a custom designed MATLAB program as previously described (2).

Localization of RhoH–mRFP was assessed in transiently transfected Jurkat cells at 20 min with Raji cells preloaded with SEE and labeled green with carboxy fluorescein succinimidyl ester (CFSE). Cell conjugates were tracked by contacts between antigen presenting cells (APC) and $mRFP^+$ cells and then the localization of mRFP was quantified by the frequency of conjugates displaying a diffuse localization pattern of mRFP versus mRFP recruited toward the APC. Alternatively, conjugate formation was assessed by performing a flow-based conjugate assay as previously described (3). T cells and prepulsed APC($^{-/+}$ $OVA_{323–339}$) for 1 h at 37 °C were mixed at a 1:1 ratio, either unstimulated (NoAg) or stimulated (+Ag) and incubated for various time points. Antigen dose–response curves started a 1 μg/mL, fourfold dilutions to 0.0019 μg/mL. Subsequently, cell surface staining for CD4 and B220 was performed followed by fixation, washing, and flow cytometry. Conjugate frequencies were determined from the percentage of transfected cells that were $CD4^+B220^+$ doublets relative to the total number of transfected $CD4^+$ cells.

**Competitive Homing Assays.** Competitive homing assays were performed similar to other reports (4). Naïve CD4 T cells from WT (National Cancer Institute) and RhoH-deficient mice (5) were sorted for $CD4^+$ $CD44^{low}$, labeled with PKH26 and CFSE, respectively, or vice versa, and i.v. injected into WT recipient mice in a 1:1 ratio. $CD4^+$ live cells from blood, peripheral and mesenteric lymph nodes, bone marrow, and spleen were assessed a day later or mice were treated with FTY720 or anti-CD62L at this time and harvested 12–20 h later. The effectiveness of FTY720 treatment is confirmed by a reduction in the number of CD4 T cells found in the circulation (4).

**RT-PCR.** CFSE-labeled mouse CD4 T cells were stimulated with plate bound CD3 (1 mg/mL) and CD28 (2 mg/mL) for 4–6 d and sorted by $CD4^+$ and CFSE dilutions. Alternatively OT-II transgenic T cells were stimulated with $OVA_{323–339}$ presented by irradiated splenocytes from RhoH-deficient mice. RNA was isolated by Trizol extraction as previously described (6) and cDNA synthesis was done per manufacturer protocol. Samples were run on an Applied Biosystems Prism 7700 Sequence BioDetector.


1. Morin NA, et al. (2008) Nonmuscle myosin heavy chain IIA mediates integrin LFA-1 de-adhesion during T lymphocyte migration. *J Exp Med* 205:195–205.
2. Hyun YM, Chung HL, McGrath JL, Waugh RE, Kim M (2009) Activated integrin VLA-4 localizes to the lamellipodia and mediates T cell migration on VCAM-1. *J Immunol* 183: 359–369.
3. Morgan MM, et al. (2001) Superantigen-induced T cell:B cell conjugation is mediated by LFA-1 and requires signaling through Lck, but not ZAP-70. *J Immunol* 167:5708–5718.
4. Pham TH, Okada T, Matloubian M, Lo CG, Cyster JG (2008) S1P1 receptor signaling overrides retention mediated by G alpha i-coupled receptors to promote T cell egress. *Immunity* 28:122–133.
5. Dorn T, et al. (2007) RhoH is important for positive thymocyte selection and T-cell receptor signaling. *Blood* 109:2346–2355.
6. Sanchez-Lockhart M, et al. (2004) Cutting edge: CD28-mediated transcriptional and posttranscriptional regulation of IL-2 expression are controlled through different signaling pathways. *J Immunol* 173:7120–7124.


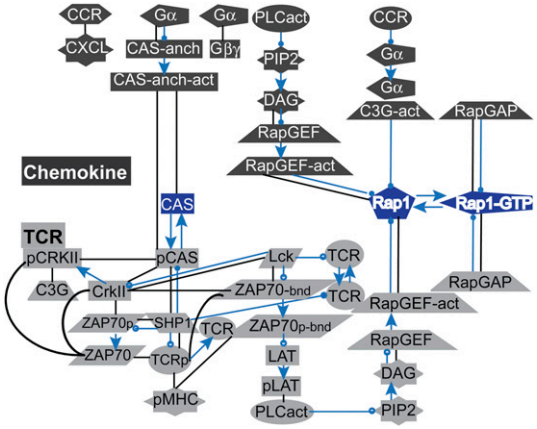


**Fig. S1.** The small GTPase, Rap1, is a key regulator of LFA-1–mediated adhesion induced by TCR or chemokine receptor. The Simmune modeling program was used to assess key points of overlap in the signaling pathways downstream of chemokine-receptor or TCR activation. Chemokine-induced signaling pathways are color-coded black, whereas TCR-related pathways are gray. A line with a circle represents the action of an enzyme on its substrate. A line with an arrow indicates the transformation of the substrate into the product of the reaction. Black lines represent those passive binding possibilities that play important roles for the regulation of protein activity. CAS and Rap1, key points of overlap between the intracellular signal cascades, are denoted in blue.

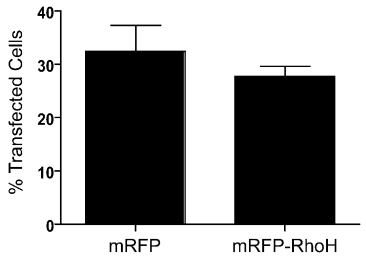


**Fig. S2.** Quantitation of transient transfection of Jurkat cells. Jurkat cells transiently transfected with mRFP or RhoH–mRFP were imaged for DIC and mRFP signal. Manual counting of total cells versus $mRFP^+$ cells were performed. Data are means ± SEM, $n = 3$.

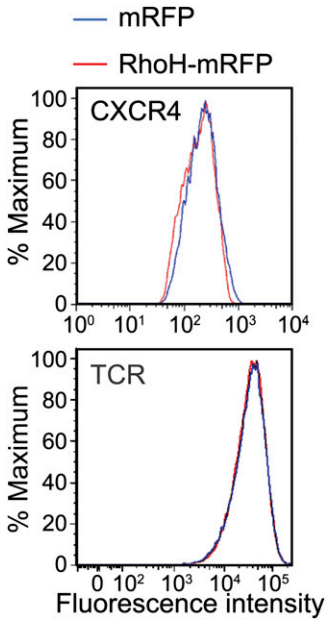


**Fig. S3.** Transient RhoH overexpression does not alter surface levels of CXCR4 or TCR. Representative flow cytometry histogram plots of cell surface levels of CXCR4 and TCR are shown from Jurkat cells transiently transfected with mRFP or RhoH–mRFP.

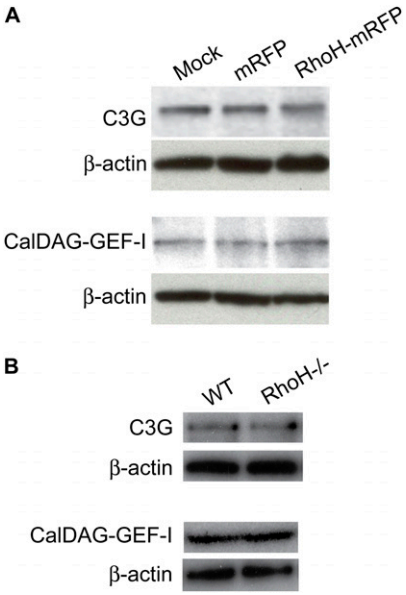


**Fig. S4.** Overexpression or deficiency of RhoH does not alter the endogenous levels of C3G or CalDAG–GEFI. (*A* and *B*) Representative blots of C3G and CalDAG–GEFI from stable Jurkat cell lines or parental line (*A*) or RhoH$^{-/-}$ and WT murine T cells (*B*) are shown.

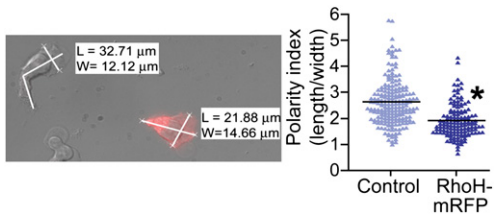


**Fig. S5.** RhoH-overexpressing cells displayed a polarized morphology with relatively short tails compared with control cells. (*A*) Representative image of control and RhoH–mRFP expressing cell with lines indicating the length and width of each cell. The polarization index was calculated by dividing the length by width for individual cells, $n = 3$ (35–81 cells in each) $P < 0.0001$ by Student's *t*-test.

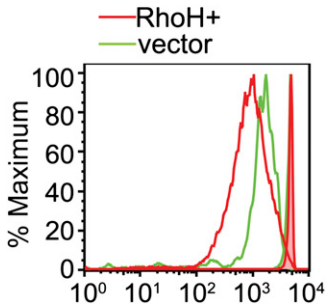


**Fig. S6.** RhoH-overexpressing cells dilute more PKH compared with control cells. Sorted retrovirally transduced cells were labeled with PKH26 and stimulated with Ag. Undivided cells were assessed on day 1 (shaded histograms) and then dilution of PKH was assessed on day 3 (open histograms). As the retrovirally transduced cells express $GFP^+$ it was necessary to use PKH dilution; yet PKH fails to give distinct division peaks. RhoH-overexpressing cells dilute more PKH, suggesting that these cells may be progressing through an activation program at a faster rate. Representative plot of three independent cell populations for each.

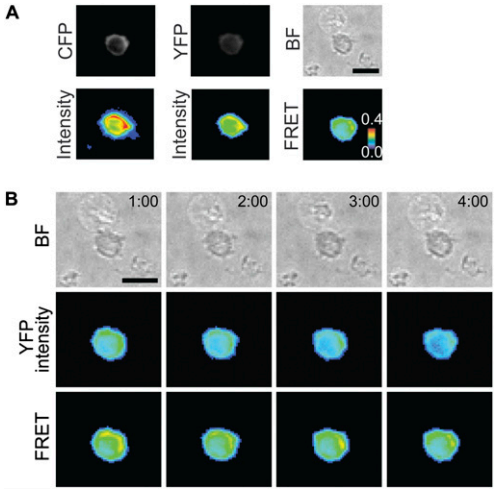


**Fig. S7.** Basal Rap1 activation in the absence of chemokine. (*A* and *B*, Movie S3) Human T-cell blasts were transiently transfected with Raichu–Rap1 FRET sensor, then allowed to interact on ICAM-1–coated coverslips. CFP and YFP images are shown in gray and corresponding color scaled intensity plots are below. FRET efficiency is shown in rainbow colors, highest (red) to lowest (blue). (*B*) Representative cells dynamic Rap1 FRET at select time points in control conditions of ICAM-1–only coated surface.

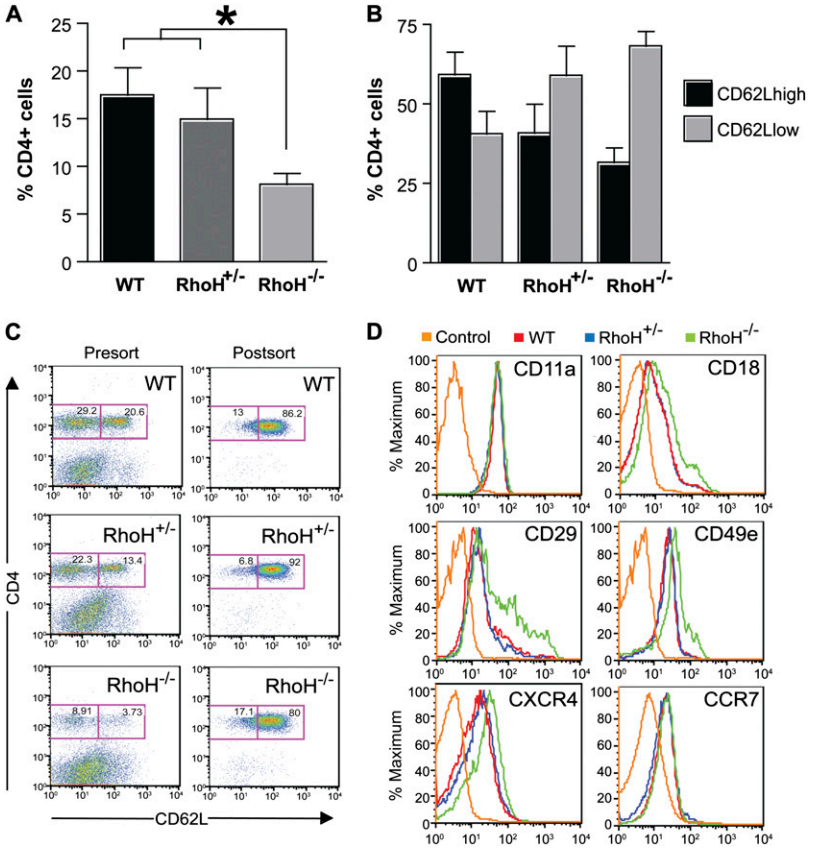


**Fig. S8.** Similar expression of key integrin and chemokine receptors on naïve T cells from WT, RhoH$^{+/-}$, and RhoH$^{-/-}$ mice. (*A*) Percentage of CD4 cells in lymph node homogenate is significantly reduced in RhoH$^{-/-}$ mice as seen by CD4 flow cytometry. (*B*) Frequency of CD62L$^{high}$ naïve T cells is significantly reduced in RhoH$^{-/-}$ mice. These data are means ± SEM, $n = 6$ and are statistically significant, $P < 0.008$. (*C*) Naïve cells sorted by CD4$^{+}$CD44$^{low}$ were stained for CD62L expression to verify equivalent expression of CD62L. (*D*) Expression of CD11a, CD18, CD29, CD49e, CXCR4, and CCR7 (by CCL-19Fc) were assessed on naïve cells from WT, RhoH$^{+/-}$, and RhoH$^{-/-}$ mice. Representative plots of $n = 3$ for WT and RhoH$^{-/-}$, $n = 2$ for RhoH$^{+/-}$.

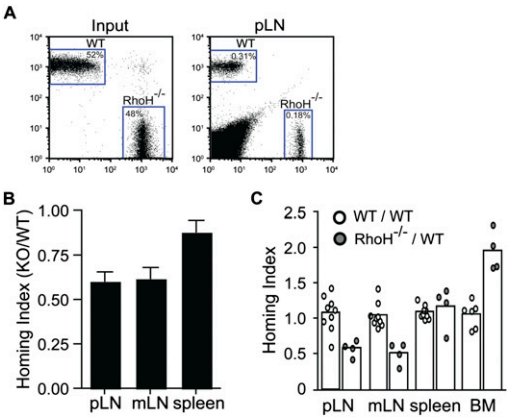


**Fig. S9.** RhoH$^{-/-}$ cells have altered homing among lymphoid tissues, which may be due to faster transit times such that RhoH$^{-/-}$ cells enter and depart lymph nodes more quickly. (*A*) Representative flow cytometry plots of input cell mixture and lymph node after transfer of labeled WT and RhoH$^{-/-}$ cells. (*B*) Ratio of RhoH$^{-/-}$/WT cells 1 d posttransfer. Data are means ± SEM, $n = 4$ experiments with 17 mice total. (*C*) Ratio of WT/WT or RhoH$^{-/-}$/WT cells 1 d posttransfer. BM, bone marrow, pLN, peripheral lymph node, mLN, mesenteric lymph node. These data are means ± SEM, $n \geq 4$ mice in one experiment.

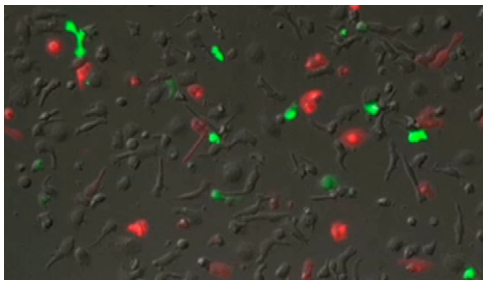

**Movie S1.** RhoH–mRFP and GFP expressing human T cells migrating on ICAM-1/CXCL12–coated surface. Transiently transfected Jurkat cells, RhoH–mRFP (red), and GFP (green) were allowed to begin migration and then migration was imaged over time at 37 °C and conditions to limit phototoxicity.

Movie S1

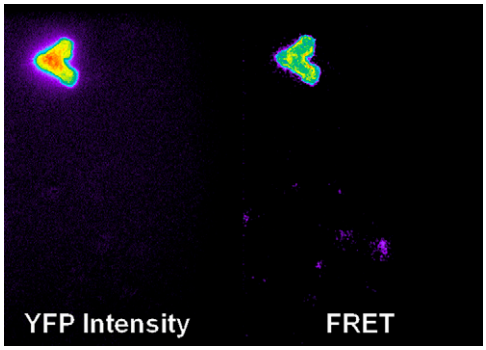


**Movie S2.** Dynamic FRET indicating active Rap1 in T-cell migrating on ICAM-1/CXCL12–coated surface. Human T-cell blasts transiently transfected with Raichu–Rap1 FRET sensor were allowed to migrate on ICAM-1/CXCL12–coated coverslips. YFP intensity (*Lower Left*) and FRET (*Lower Right*) are shown in rainbow colors, highest (red) to lowest (blue).

Movie S2

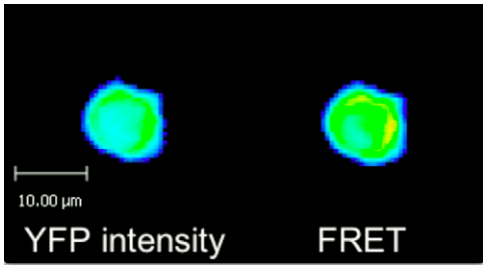


**Movie S3.** Dynamic FRET of active Rap1 in T-cell on ICAM-1–only coated surface. Human T-cell blasts transiently transfected with Raichu–Rap1 FRET sensor were allowed to migrate on ICAM-1–coated coverslips. YFP intensity (*Lower Left*) and FRET (*Lower Right*) are shown in rainbow colors, highest (red) to lowest (blue).

Movie S3

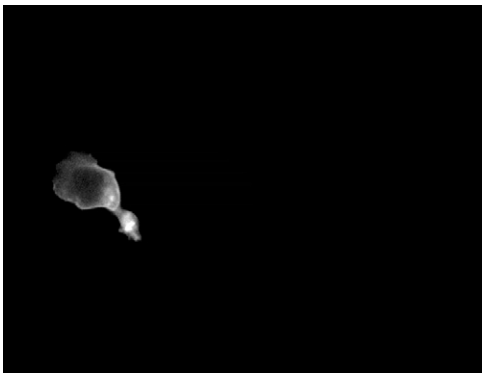

**Movie S4.** Dynamic localization of RhoH–mRFP during human T-cell migration. Transiently transfected human T-cell blasts were allowed to migrate on ICAM-1/CXCL12–coated surface. The localization of RhoH–mRFP is shown for a representative cell over time with the brighter signal indicating higher fluorescence intensity.

Movie S4

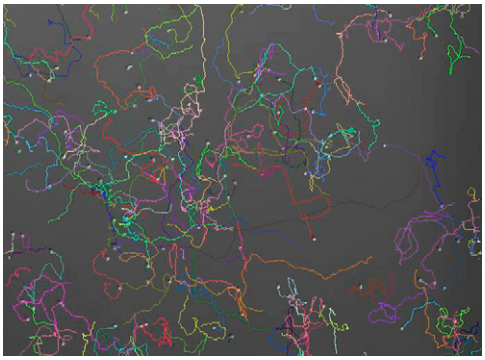

**Movie S5.** Migration of naïve WT $CD4^+$ T cells on ICAM-1/CCL21–coated surface. Sorted T cells were allowed to begin migration and then time-lapse image collection of DIC every 5 s for 10 min was collected. Migration tracks are overlaid onto video and floating cells were excluded in our analysis.

Movie S5

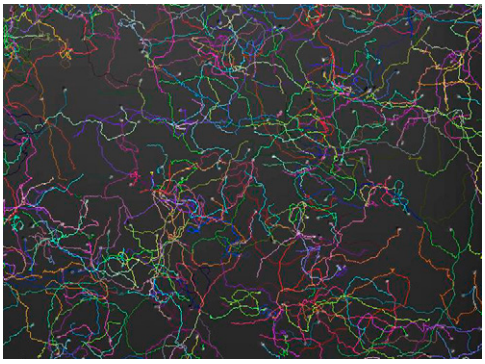

**Movie S6.** Migration of naïve $RhoH^{-/-}CD4^+$ T cells on ICAM-1/CCL21–coated surface. Sorted T cells were allowed to begin migration and then time-lapse image collection of DIC every 5 s for 10 min was collected. Migration tracks are overlaid onto video and floating cells were excluded in our analysis.

Movie S6